Optical and Structural Investigations on Mn-Ion States in MOCVD-grown $Ga_{1-x}Mn_xN$

Strassburg, Martin [1,2], Senawiratne, Jayantha [1], Hums, Christoph [1,4], Dietz, Nikolaus [1], Kane, Matthew H. [2,3], Asghar, Ali [2], Summers, Christopher J. [3], Haboeck, Ute [4], Hoffmann, Axel [4], Azamat, Dmitry [4], and Gehlhoff, Wolfgang [4], Ferguson, Ian T. [2]

[1] *Georgia State University, Department of Physics and Astronomy, Atlanta, GA 30303, U.S.A.*
[2] *Georgia Institute of Technology, School of Electrical and Computer Engineering, Atlanta, GA 30332-0250, U.S.A.*
[3] *Georgia Institute of Technology, Materials Science and Engineering, Atlanta, GA 30332-245, U.S.A.*
[4] *Institut für Festkörperphysik, Technische Universität Berlin, D - 10623 Berlin, Germany.*

ABSTRACT

The incorporation of Mn into GaMnN epilayers by MOCVD growth was investigated. Samples with high Mn concentrations lead to room temperature ferromagnetism. In addition an absorption band around 1.5 eV was observed. Intensity and linewidth of this band scaled with the Mn concentration and with the room temperature (RT) saturation magnetization. This band is assigned to the internal Mn^{3+} transition between the ^5E and the partially filled $^5T_2$ levels of the ^5D state. The broadening of the absorption band is introduced by the high Mn concentration. Recharging of the Mn^{3+} to Mn^{2+} was found to effectively suppress these transitions resulting also in a significant reduction of the RT magnetization. The pronounced sensitivity of the relative position of the Fermi level and 1.5 eV absorption band can be used to predict the magnetization behavior of the $Ga_{1-x}Mn_xN$ epilayers. The absence of doping-induced strain was observed by Raman spectroscopy. The structural quality, the presence of Mn^{2+} ions were confirmed by EPR spectroscopy, meanwhile no Mn-Mn interactions were observed.

INTRODUCTION

Recent predictions and the subsequent experimental confirmations of room temperature ferromagnetism in transition metal (TM) doped wide bandgap materials, such as $Ga_{1-x}Mn_xN$ has renewed interest in this subject area [1]. In order to make use of these materials for spintronic applications a free carrier-mediated ferromagnetism is to be achieved; however, the origin of ferromagnetism in $Ga_{1-x}Mn_xN$ and related materials is controversial as is discussed below. It has been predicted that ferromagnetism is facilitated by the interaction between the Mn^{2+} ions and the holes in the GaN valence band [1]. Preparation of p-type material would be required to shift the Fermi level in GaN towards the valence band [2]. Other theoretical predictions suggest that a Mn-induced impurity band provides a mechanism for effective-mass transport that can be exploited for carrier mediation [3,4]. Sato et al. [4] showed that the incorporation of Mn facilitates the formation of a sharp ^5E impurity band and a broader $^5T_2$ impurity band altering the electronic structure in the bandgap of $Ga_{1-x}Mn_xN$. The broadening in the partially filled $^5T_2$ band stabilizes the ferromagnetism via the double exchange interaction [5,6] provided the Fermi level is in this defect band.

In this work the experimental identification of the Mn ion charge state and the presence of bands in the bandgap of GaN is investigated by optical spectroscopy and electron spin paramagnetic resonance (EPR) [2,7,8,9]. Photoluminescence emission bands in the blue (~3 eV)

have been observed in MOCVD-grown and Mn-implanted GaN:Mn [10,11,12,13]. This provides information on defects and disorder induced impurity states by the Mn incorporation in GaN. Additional information about the position of the Fermi-level and the existence of an impurity band was obtained using absorption spectroscopy revealing energy states around 1.1 eV, 1.5 eV and 1.8 eV. These states were assigned to interatomic transitions or to transitions between the Mn-states and the valence band, or to both [2,8,9].

In this paper, an investigation of the Fermi level dependence of the optical and structural properties of $Ga_{1-x}Mn_xN$ with room temperature magnetization behavior is presented. MOCVD growth was applied in order to increase the concentration of Mn incorporated on Ga sites in the desired charge state (Mn^{2+}) to support the ferromagnetism while maintaining the diluted magnetic semiconductor properties. Broadening of the $^5T_2$ state according to the high Mn concentration was confirmed by a broad absorption band detected around 1.5 eV. Its linewidth and magnitude scaled with the Mn concentration, and showed a strong dependence on the position of the Fermi-level that was in addition varied by silicon co-doping and/or annealing. No strain and no significant concentration of free carriers were introduced by Mn alloying as confirmed by Raman spectroscopy. This was consistent with electrical measurements that showed the as grown material to highly resistive. These results suggest that a double exchange interaction is the most likely mechanism for ferromagnetism in $Ga_{1-x}Mn_xN$.

EXPERIMENTAL DETAILS

GaMnN films with Mn concentration up to ~2.3% were grown by MOCVD at temperatures above 1000 °C. The MOCVD tool is an EMCORE discovery series D-125 GaN tool with a vertical injection system into a short jar confine inlet design. The tool gives the option of running N_2 and H_2 as carrier gas for all MO sources. Ammonia, tri-methyl gallium, Bis-cyclopentadienyl manganese (Cp_2Mn), bis-cyclopentadienyl magnesium (Cp_2Mg) and silane (SiH_4) were used as the nitrogen, gallium, manganese, p-, and n-dopant sources, respectively, for the GaMnN. The GaMnN films were typically ~500 nm thick grown on sapphire and had a reddish tinge to them. Subsequent characterization of these films was performed, including X-ray diffraction (XRD), secondary ion mass spectroscopy (SIMS), atomic force microscopy (AFM) and SQUID magnetometry measurements. SIMS confirmed homogeneous Mn incorporation and no second phases (e.g., Mn_xN_y) were observed in XRD. All the GaMnN samples showed room temperature magnetism except for the highest Si concentrations $> 10^{19}\,cm^{-3}$. The magnetic properties are described in detail elsewhere [14,15,16].

Photoluminescence (PL) data was obtained using a frequency-doubled Titanium-Sapphire laser and transmission measurements were performed using the red and infrared spectrum of a halogen lamp. The emitted and transmitted light was detected by a photomultiplier attached to a 0.24 m monochromator with a spectral resolution of better than 1 nm for emission and better than 6 nm for transmission experiments which is adequate for the broad band transitions investigated in this work.

RESULTS AND DISCUSSION

Optical and structural measurements have been used to investigate the origin of the room temperature (RT) ferromagnetism (FM) observed in GaMnN epilayers. A detailed description of the magnetization behavior is given elsewhere but will referenced as needed [14,15,16]. In

general, RT FM scaled with the Mn concentration. RT FM was also observed, but significantly weaker, in MOCVD-grown semi-insulating and n-type epilayers. FM could be completely suppressed when co-doping with $> 10^{19-20}$ cm^{-3} silicon atoms. This indicates that the RT FM is very sensitive to the position of the Fermi level in order that the Mn ion is in the Mn^{3+} state; however, the magnetization data alone do not provide enough information to reveal the actual origin of the RT FM.

Electron paramagnetic resonance (EPR) in the X band was used to study the incorporation and the electronic structure of the Mn ions in GaN. In the X band only the typical spectra of isolated Mn^{2+} were observed. The characteristic EPR spectra of a ~1 µm thick Ga$_{0.978}$Mn$_{0.022}$N epilayers co-doped with silicon ([Si] = 2e19cm^{-3}) for the magnetic field directions B parallel and perpendicular to the hexagonal crystal axis c are shown in Figure 1(a) together with the corresponding stick spectra. The allowed five fine structure lines generated by the electron spin transitions with $\Delta M = \pm 1$ are resolved, each six fold split by the ^{55}Mn hyperfine interaction due to the coupling of the $^6A_1$ ground state of Mn^{2+} to the nuclear spin I=5/2 of the natural isotope ^{55}Mn. No allowed EPR transition within the Mn^{3+} ground state manifold with S=2 could be observed in the X-band with the available magnetic field. The acceptor states and the compensation mechanism are investigated in more detail by PL and absorption spectroscopy, presented later in this paper.

Significant strain or deviations from crystalline symmetry can be ruled out according to the observed small line broadening of the outer fine-structure lines by rotation of the magnetic field B in different crystallographic planes. This conclusion is supported by the determined fine-structure parameter D = -230x10^{-4} cm^{-1} which is similar to that obtained for strain-relieved MBE grown GaN:Mn layers [17]). Furthermore, the isotropic g factor and the isotropic hyperfine parameter A are identical with the values found for Mn-doped GaN-films grown by MBE [17].
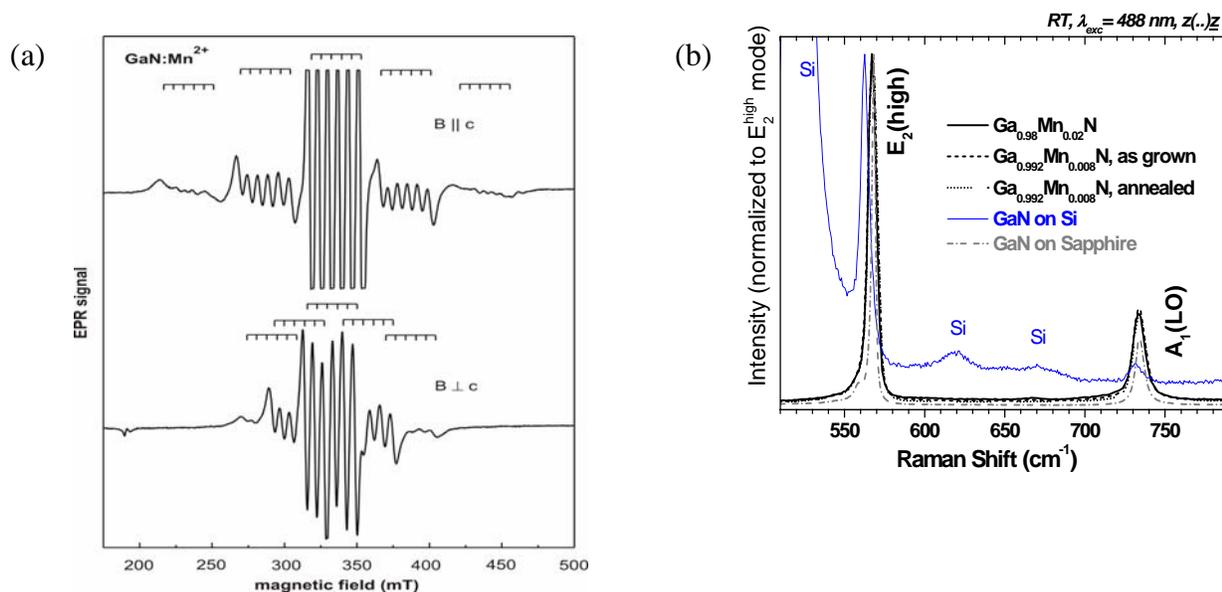
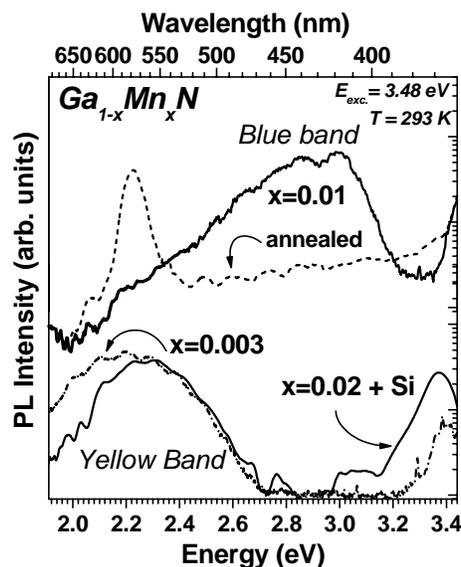**Figure 1.** (a) EPR spectra of as deposited Ga$_{0.978}$Mn$_{0.022}$N:Si recorded in magnetic fields parallel and perpendicular to the c-axis at 5K. The presence of Mn^{2+} ions in GaN is unambiguously proven by the hyperfine resonances. (b) Raman spectra of MOCVD-grown GaN epilayers with different Mn concentrations and sample preparation. For comparison, GaN epilayers grown on sapphire and on Si substrates are also shown. The strain induced by the stronger lattice and thermal mismatch of Si substrates lead to a red shift of the Raman modes in this case.

The absence of Mn-induced strain was also confirmed by micro-Raman investigations. Raman spectra of GaMnN with different Mn and carrier concentrations are presented in Figure 1(b). Raman spectra of GaN epilayers grown on sapphire and on silicon are shown for comparison. Most prominent in all these spectra are the E_2 high and the A_1 (LO) Raman modes that were detected at 567 cm^{-1} and 734 cm^{-1}, respectively. These values are in good agreement with those measured for relaxed GaN revealing that no additional strain was introduced even though a high concentration of Mn ions (~10^{20} cm^{-3}) was incorporated in the GaN. A high carrier concentration (above 10^{18} cm^{-3}) was ruled out since no broadening of the A_1 mode and no LLP modes were detected. According to the stronger strain in the case of the Si substrate, the Raman modes of this sample are shifted to lower energies compared with the epilayers on sapphire.
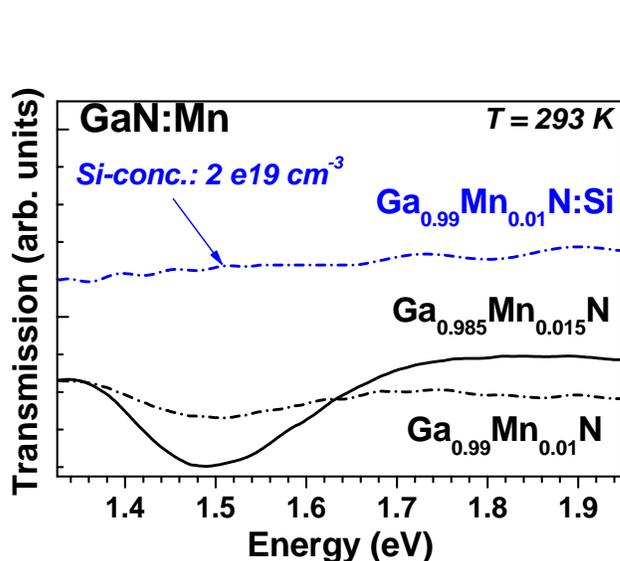
Figure 2. Transmission spectra of $Ga_{1-x}Mn_xN$ with varying Mn concentrations. In addition, a transmission spectrum of a co-doped $Ga_{1-x}Mn_xN$:Si sample is shown. The spectrum of the Si co-doped sample is vertically shifted for clarity.

Figure 3 Photoluminescence spectra of GaMnN recorded in the visible and UV spectral range.

In order to reveal the charge state of the incorporated Mn ions incorporated in GaN, both transmission and emission studies were performed. The transmission spectra of two samples differing in their Mn content are shown in Figure 2. The incorporation of Mn into GaN layers during MOCVD growth leads to a broad absorption band (dip in transition spectra) and a spectrally diffuse line around 1.5 eV with a larger linewidth (full width at half of maximum – FWHM) as it was observed in MBE-grown and implanted GaMnN epilayers [2,9]. The relatively large FWHM of ~150 meV for this absorption band and an increase of its FWHM and intensity with increasing Mn concentration were observed. Mn^{3+} transitions Mn^{3+} transitions from the E state to the partially filled T_2 levels of the ^5D state are assigned to the observed absorption band and broadened due to the high Mn concentration [4]. The transmission of the third sample, shown in Figure 2, was prepared to exhibit n-type behavior by co-doping with silicon during growth. Hall measurements showed a slight increase in the free electron density in the conduction band (at RT). This behavior is attributed to the (over-) compensation of Mn

acceptor states due to the trapping of the Si donor electrons. The absence of the absorption band around 1.5 eV in the $Ga_{1-x}Mn_xN$ layer co-doped with silicon points towards its sensitivity to the position of the Fermi level. The Fermi level is shifted towards the conduction band because electrons are present at deep defects. No other absorption features were detected further in the infrared spectral range (down to 0.5 eV). This suggests that the location of the Fermi level in the investigated samples in the broad absorption band is around 1.8 eV above the valence band energy, and even closer to the conduction band than for the Si co-doped sample. However, an unambiguous proof that this Mn-induced band is the magnetism for RT FM is still needed and could be addressed by spin-sensitive spectroscopic techniques.

In order to further understand the ferromagnetic nature and Mn-induced midgap states of MOCVD-grown $Ga_{1-x}Mn_xN$ epilayers PL studies were performed in the UV and visible spectral range. The RT PL of various samples are shown in Figure 3: three as-grown samples differing in Mn concentration and one annealed sample with a Mn concentration of 1%. The blue emission band was found to govern the PL spectrum of the samples with a manganese concentration >0.5 % resulting in two distinct peaks at 3.0 eV and 2.8 eV. The band at 3.0 eV is attributed to Mn-related or Mn-induced transitions for heavily Mn doped samples. Recently, the blue band emission was observed in MBE-grown GaMnN [18], and the appearance of these bands was assigned to transitions from conduction band electrons to Mn - related states and from shallow donor (e.g., N vacancy) to Mn acceptor states [10,11,12,13]. In comparison, almost no blue band emission but a pronounced yellow band attributed to intrinsic gallium defects was observed in the lightly doped GaMnN samples (<0.5%) [17], the annealed sample and the sample co-doped with Si. In the first case, the behavior is assigned to the lower amount of Mn ion available to substitute on lattice site reducing the amount of Ga vacancies. In the latter two cases, intrinsic and extrinsic shallow donor states are introduced leading to a recharging of the Mn^{3+} acceptors. This is in agreement with the reduced intensity of the absorption band around 1.5 eV that was found to decrease also by decreasing the Mn concentration and as a result of annealing. An even stronger compensation of Mn acceptors is seen for Si co-doping. The PL is similar to that found for GaMnN with low Mn concentration and hence, a strong reduction in the intensity of the Mn-related blue band emission around 3.0 eV was observed.

CONCLUSION

High concentrations of Mn on Ga site (between 0.3% and 2 %) were incorporated in $Ga_{1-x}Mn_xN$ by MOCVD growth. According to the high Mn concentration, the T_2 states of the Mn 3d shell were broadened. This broadening was confirmed by the observation of a respective absorption band around 1.5 eV related to inner ^5D state transitions (T_2 to E) of Mn ions. This absorption scaled with the Mn concentration. In contrast, this band vanished when the concentration of free electrons was increased (e.g., by Si co-doping and by annealing) leading to the compensation of the partially filled T_2 band that equals the transition from the Mn^{3+} to the Mn^{2+} state. In this case, also the saturation magnetization decreased confirming the Fermi-level dependence of the ferromagnetism.

ACKNOWLEDGMENTS

REFERENCES

1 T. Dietl, H. Ohno, F. Matsukura, J. Cibert, and D. Ferrand, Science **287**, 1019-1022 (2000).
2 E.g., T. Graf, M. Gjukic, M. S. Brandt, M. Stutzmann, and O. Ambacher, Appl. Phys. Lett. **81**, 5159-5161 (2002).
3 L. Kronik, M. Jain, and J. R. Chelikowsky, Phys. Rev. B **66**, 041203 (2002).
4 K. Sato, P. H. Dederichs, H. Katayama-Yoshida, J. Kudrnovsky, Physica B 340–**342**, 863–869 (2003).
5 H. Akai, Phys. Rev. Lett. **81**, 3002 (1998).
6 K. Sato, H. Katayama-Yoshida, Semicond. Sci. Technol. **17**, 367 (2002).
7 A. Wolos, M. Palczewska, M. Zajac, J. Gosk, M. Kaminska, A. Twardowski, M. Bockowski, I. Grzegory, and S. Porowski, Physical Review B **69**, 115210 (2004).
8 R. Y. Korotkov, J. M. Gregie, B. W. Wessels, Appl. Phys. Lett. **80**, 1731 (2002).
9 O. Gelhausen, E. Malguth, M. R. Phillips, E. M. Goldys, M. Strassburg, A. Hoffmann, T. Graf, M. Gjukic, M. Stutzmann, Appl. Phys. Lett. **84**, 4514 (2004).
10 Yoon Shon, Young Hae Kwon, Sh. U. Yuldashev, J. H. Leem, C. S. Park, D. J. Fu, H. J. Kim, T. W. Kang, and X. J. Fan, Appl. Phys. Lett. **81**, 1845 (2002).; Yoon Shon, Young Hae Kwon, Sh. U. Yuldashev, Y. S. Park, D. J. Fu, D. Y. Kim, H. S. Kim, and T. W. Kang, J. Appl. Phys. **93**, 1546 (2003).
11 J. Xu, J. Li; R. Zhang, X.Q. Xiu, D.Q. Lu, S.L. Gu, B. Shen, Y. Shi, Y.D. Zheng, Mat. Res. Soc. Symp. Proceedings **693**, 207 (2002).
12 A. Y. Polyakov, N. B. Smirnov, A. V. Govorkov, N. Y. Pashkova, J. Kim, F. Ren, M. E. Overberg, G. T. Thaler, C. R. Abernathy, S. J. Pearton, and R. G. Wilson, J. of Appl. Phys. **92,** 3130-3135 (2002).
13 J. M. Baik, J.-L. Lee, Y. Shon, and T. W. Kang, J. Appl. Phys. **93**, 9024 (2003).
14 M.H. Kane, A. Asghar, A.M. Payne, C.R. Vestal, M. Strassburg, J. Senawiratne, Z.J. Zhang, N. Dietz, C.J. Summers, I.T. Ferguson, Surf. Sc. & Technol., accepted for publication (2004).
15 M. Strassburg, M.H. Kane, A. Asghar, C.R. Vestal, Z.J. Zhang, J. Senawiratne, M. Alevli, N. Dietz, C.J. Summers, I.T. Ferguson, to be published in Phys. Rev. B rapids (2004).
16 Matthew H. Kane, Ali Asghar, Adam M. Payne, Ian T. Ferguson, Christopher R. Summers, Christy R. Vestal, Z. John Zhang, Martin Strassburg, Jayantha Senawiratne, Nikolaus Dietz, Dmitry Azamat, Ute Haboeck, Axel Hoffmann, and Wolfgang Gehlhoff, Proc. of the MRS fall meeting (2004), this volume.
17 T. Graf et al., Phys. Rev. B67, 165215 (2003).
18 Y. L. Soo, S. Kim, Y. H. Kao, A. J. Blattner, B. W. Wessels, S. Khalid, C. Sanchez Hanke, and C.-C. Kao, Applied Physics Letters **84,** 481-483 (2004).